Available online at www.sciencedirect.com

ScienceDirect

journal homepage: www.JournalofSurgicalResearch.com

Antiapoptotic Effect by PAR-1 Antagonist Protects Mouse Liver Against Ischemia-Reperfusion Injury

Daisuke Noguchi, MD, Naohisa Kuriyama, MD, Takahiro Ito, MD, Takehiro Fujii, MD, Hiroyuki Kato, MD, Shugo Mizuno, MD, Hiroyuki Sakurai, MD, and Shuji Isaji, MD*

Department of Hepatobiliary Pancreatic and Transplant Surgery, Mie University Graduate School of Medicine, Tsu, Mie, Japan

ARTICLE INFO

Article history:
Received 28 May 2019
Received in revised form
30 August 2019
Accepted 19 September 2019
Available online xxx

Keywords:
Protease-activated receptor-1
Hepatic ischemia-reperfusion injury
SCH530348
Apoptosis
Extracellular signal–regulated kinase 1/2

ABSTRACT

Background: Coagulation disturbances in several liver diseases lead to thrombin generation, which triggers intracellular injury via activation of protease-activated receptor-1 (PAR-1). Little is known about the thrombin/PAR-1 pathway in hepatic ischemia-reperfusion injury (IRI). The present study aimed to clarify whether a newly selective PAR-1 antagonist, vorapaxar, can attenuate liver damage caused by hepatic IRI, with a focus on apoptosis and the survival-signaling pathway.

Methods: A 60-min hepatic partial-warm IRI model was used to evaluate PAR-1 expression *in vivo*. Subsequently, IRI mice were treated with or without vorapaxar (with vehicle). In addition, hepatic sinusoidal endothelial cells (SECs) pretreated with or without vorapaxar (with vehicle) were incubated during hypoxia-reoxygenation *in vitro*.

Results: In naïve livers, PAR-1 was confirmed by immunohistochemistry and immunofluorescence analysis to be located on hepatic SECs, and IRI strongly enhanced PAR-1 expression. In IRI mice models, vorapaxar treatment significantly decreased serum transaminase levels, improved liver histological damage, reduced the number of apoptotic cells as evaluated by terminal deoxynucleotidyl transferase dUTP nick end labeling staining (median: 135 *versus* 25, $P = 0.004$), and induced extracellular signal-regulated kinase 1/2 (ERK 1/2) cell survival signaling (phospho-ERK/total ERK 1/2: 0.96 *versus* 5.34, $P = 0.004$). Pretreatment of SECs with vorapaxar significantly attenuated apoptosis and induced phosphorylation of ERK 1/2 *in vitro* (phospho-ERK/total ERK 1/2: 0.66 *versus* 3.04, $P = 0.009$). These changes were abolished by the addition of PD98059, the ERK 1/2 pathway inhibitor, before treatment with vorapaxar.

Conclusions: The results of the present study revealed that hepatic IRI induces significant enhancement of PAR-1 expression on SECs, which may be associated with suppression of survival signaling pathways such as ERK 1/2, resulting in severe apoptosis-induced hepatic damage. Thus, the selective PAR-1 antagonist attenuates hepatic IRI through an antiapoptotic effect by the activation of survival-signaling pathways.

* *Corresponding author*. Department of Hepatobiliary Pancreatic and Transplant Surgery, Mie University Graduate School of Medicine, Edobashi 2-174, Tsu, Mie, Japan. Tel.: +81 59-232-1111; fax: +81 59-232-8095.
E-mail address: naokun@clin.medic.mie-u.ac.jp (N. Kuriyama).

0022-4804/$ – see front matter
https://doi.org/10.1016/j.jss.2019.09.044

Introduction

Hepatic ischemia-reperfusion injury (IRI) is a serious cause of liver damage that occurs during liver resection and transplantation.[1] Multiple mediators and signaling pathways contribute to the pathophysiology of hepatic IRI and cause direct cellular injury as a result of inflammation and apoptotic cell death.[2,3] Because the liver is responsible for the synthesis of the majority of coagulation factors,[4] liver failure caused by several diseases, including hepatic IRI, results in significant changes to the hemostatic system. Indeed, some studies have shown that the development of hepatocellular injuries in acute and chronic liver diseases such as obstructive jaundice and nonalcoholic fatty liver disease is associated with the activation of the blood coagulation cascade.[5-7] Coagulation cascade activation results in the generation of thrombin, a pluripotent serine protease, which triggers intracellular signaling in numerous cells through the activation of protease-activated receptor-1 (PAR-1),[8] causing inflammation, apoptotic cell death, and cellular injury.[9-11]

PAR-1, a member of a large family of seven transmembrane domain G-protein–coupled receptors, was first identified as a major high-affinity receptor of thrombin.[12] Because PAR-1 is also activated by activated protein C (APC),[13] PAR-1 elicits paradoxical signaling responses depending on whether it is activated by thrombin or APC. In the signaling bias of PAR-1, thrombin induces proinflammatory and proapoptotic signaling,[14-16] whereas APC evokes anti-inflammatory and cytoprotective responses.[17-19] In our institution, we previously investigated the cytoprotective effects of APC-activated PAR-1 signaling in hepatic IRI models. We found that a liver preservation solution containing APC was a potential novel and safe product for small-for-size liver transplantation,[20] and that APC in steatotic liver attenuated late-phase damage caused by hepatic IRI via activation of adenosine monophosphate–activated protein kinase.[21] Recently, Ito *et al.*[22] further explored signaling through sphingosine-1-phosphate receptor 1, which is a receptor located downstream of the APC-activated PAR-1 pathway, and demonstrated that a sphingosine-1-phosphate receptor 1 agonist attenuated hepatic IRI by protecting sinusoidal endothelial cells (SECs). However, comparative studies on the catalytic efficiency of PAR-1 activation have revealed that APC is 1×10^4 fold less potent than thrombin; therefore, thrombin has been regarded as the dominant activator of PAR-1.[23,24] This finding suggests that thrombin-activated PAR-1 signaling could be a more effective therapeutic target against hepatic IRI, that is, a selective PAR-1 as opposed to APC antagonist. In agreement with this concept, several previous studies in various IRI models, such as the kidney,[25] heart,[26] and brain,[27] reported exacerbation of IRI mediated by thrombin and/or PAR-1 activation and the protective effects of PAR-1 antagonism, including a decrease in the number of pivotal inflammatory cytokines in renal IRI,[28] a reduction of infarct size in myocardial IRI,[29] and the attenuation of p38 mitogen-activated protein kinase (MAPK) apoptotic signaling and neuronal cell death in cerebral IRI.[30] However, to our knowledge, no studies have investigated the efficacy of a PAR-1 antagonist in hepatic IRI.

Therefore, the aim of the present study was to elucidate the effect of a highly selective PAR-1 antagonist, vorapaxar, in hepatic IRI using a partial-warm IRI model of mice and an hypoxia-reoxygenation (H/R) model of hepatic SECs, paying special attention to the survival-signaling pathway, especially extracellular signal–regulated kinase 1/2 (ERK 1/2), which is involved in protection against various stressors.

Materials and methods

Animals

Eight- to nine-week-old male C57BL/6 mice (20-26 g; Japan SLC Inc, Hamamatsu, Japan) were used. The experiments were reviewed and approved by the Animal Care and Use Committee at Mie University Graduate School of Medicine (No. 28-9) and conducted in compliance with the Guidelines for Animal Experiments of Mie University Graduate School of Medicine.

Partial hepatic IRI model

A hepatic partial-warm IRI model was established in mice as previously reported.[21,22] Mice were anesthetized with isoflurane, and livers were exposed through a midline laparotomy. The arterial and portal venous blood supplies were interrupted to the cephalad lobes of the liver for 60 min using an atraumatic clip. The right hepatic and caudate lobes were perfused to prevent intestinal congestion. After 60 min of ischemia, the clip was removed, thereby initiating hepatic reperfusion. At 4 h after reperfusion, the mice were sacrificed to collect blood and liver tissues.

Measurement of serum transaminases

Serum aspartate transaminase (AST) and alanine transaminase (ALT) levels were measured using a commercially available kit (Test Wako for transaminase; Wako Pure Chemical Industries Ltd, Osaka, Japan) following the manufacturer's instructions.

Dose determination of the PAR-1 antagonist, SCH530348 (vorapaxar)

The potent and highly selective PAR-1 antagonist, SCH530348 (vorapaxar), was purchased from Selleck Chemicals (Houston, TX). Vorapaxar was dissolved in 100% dimethyl sulfoxide (DMSO), and the final DMSO concentration was 1%. The mice in our models were administrated vorapaxar intraperitoneally to stabilize absorption. In a previous study using a pulmonary infection model of mice administrated vorapaxar intraperitoneally, a cytoprotective effect was reported.[31] In addition, published pharmacokinetic data on vorapaxar administration by oral gavage in monkeys showed that a dose greater than 100 μg/kg inhibited platelet aggregation.[32] Following these data, we considered that a cytoprotective effect of vorapaxar might be expected from intraperitoneal administration and

that a dose of vorapaxar less than 100 μg/kg was more suitable for perioperative use.

To examine the effect of vorapaxar treatment in our hepatic IRI model based on serum AST levels at 4 h after reperfusion, vorapaxar was administrated intraperitoneally at 60 min before ischemia and immediately after reperfusion at several different doses ($n = 4$ in each group). As shown in Supplemental Figure 1, a dose of 5 μg/kg had a significant effect: 4236 [3688-4918] IU/L in controls *versus* 2637 [2369-2809] IU/L in the vorapaxar treatment group ($P = 0.021$). Accordingly, we decided to administer 5 μg/kg of vorapaxar.

Experimental groups of mice

All mice were randomly allocated to two IRI groups and two nonischemic controls groups as follows ($n = 6$ in each group). The IRI + vorapaxar group (IRI-1) received intraperitoneal administration of 5 μg/kg of vorapaxar, whereas the IRI + vehicle group (IRI-2) received intraperitoneal administration of vehicle (1% DMSO equivalent to that used to dissolve vorapaxar) at 60 min before ischemia and immediately after reperfusion. The mice in the IRI groups underwent the surgery described previously under the same conditions. The sham + vorapaxar group (nonischemic controls-1) received intraperitoneal administration of 5 μg/kg of vorapaxar, whereas the sham + vehicle group (nonischemic controls 2) received intraperitoneal administration of vehicle (1% DMSO equivalent to that used to dissolve vorapaxar) with the same timing as that of the IRI groups. The mice in the nonischemic control groups underwent laparotomy alone under the same conditions.

Histology

Liver specimens were fixed in a 10% buffered formalin solution, embedded in paraffin, and processed for hematoxylin and eosin staining, as previously described.[33] The histological severity of hepatic IRI was graded using a modified Suzuki's score.[34] In this classification, sinusoidal congestion, hepatocyte necrosis, and ballooning degeneration were graded from 0 to 4. No necrosis, congestion, or centrilobular ballooning was given a score of 0, whereas severe congestion, ballooning degeneration, and 60% lobular necrosis were given a score of 4. The results were evaluated by averaging 10 scores in 40 high-power fields per section in a blinded manner.

Immunohistochemistry

Liver specimens embedded in paraffin were deparaffinized and rehydrated. The monoclonal antibody against mouse PAR-1 (ATAP2; Santa Cruz, CA) was used as the primary antibody at a dilution of 1:60. Staining was carried out using the Vector Mouse on Mouse kit (Vector Laboratories, Burlingame, CA) to reduce endogenous mouse Ig staining, following the manufacturer's instructions. In Ly6G staining, liver specimens embedded in Tissue-Tek OCT compound (Miles, Elkhart, IN) and snap-frozen in liquid nitrogen were used for immunostaining, as previously described.[33] Primary antibody against Ly6G (BioLegend, San Diego, CA) was used at a dilution of 1:500. The results were evaluated by averaging 10 counts of the number of Ly6G-positive cells in 20 high-power fields per section in a blinded manner.

Immunofluorescence analysis

Liver specimens embedded in paraffin were deparaffinized and rehydrated. The monoclonal antibody against mouse PAR-1 (ATAP2; Santa Cruz, CA) at a dilution of 1:50 and the polyclonal antibody against rabbit CD31 (PECAM-1; Santa Cruz, CA) at a dilution of 1:50 were used as primary antibody. Fluorescence signals were detected by Alexa Fluor 488 (green)–labeled and Alexa Fluor 594 (red)–labeled secondary antibodies. Vectashield mounting media with DAPI (Vector Laboratories, Burlingame, CA) were used for nuclear staining. Slides were observed through the appropriate filter using a fluorescence microscope (BX51; Olympus, Tokyo, Japan).

Terminal deoxynucleotidyl transferase dUTP nick end labeling staining

Terminal deoxynucleotidyl transferase-mediated dUTP nick end labeling (TUNEL) staining was performed to evaluate apoptotic cells in both an *in vivo* study of mice ($n = 6$ in each group) and an *in vitro* study of SECs ($n = 4$ in each group) using the *In Situ* Cell Death Detection Kit (Cat No. 11684795910; Roche Diagnostics, Temecula, CA), following the manufacturer's instructions.

Paraffin-embedded liver tissue sections were deparaffinized and rehydrated, followed by 350 W microwave irradiation before the TUNEL reaction. On the other hand, SECs (1×10^5/well) were seeded and cultured overnight in a collagen-coated chamber slide (Iwaki, Tokyo, Japan). After confluence, they were exposed to H/R with or without pretreatment with vorapaxar, and fixed after the TUNEL reaction. All samples were analyzed using a fluorescence microscope (BX51; Olympus, Tokyo, Japan). The results were evaluated by averaging 10 counts of the number of TUNEL-positive cells in 20 high-power fields per section in a blinded manner.

Western blot analysis

Extraction of total protein from the whole liver or SECs and Western blot analysis were performed as previously described.[35] In brief, protein-transferred polyvinylidene fluoride membranes (EMD Millipore, Bedford, MA) were incubated overnight with specific primary antibodies against phospho-AKT (Ser473; #4060; Cell Signaling Technology, Beverly, MA), AKT (#4691; Cell Signaling Technology), phospho-ERK 1/2 (Thr202/Try204; #9101; Cell Signaling Technology), ERK 1/2 (#9102; Cell Signaling Technology), cleaved-caspase 9 (Asp330; #7237; Cell Signaling Technology), caspase 9 (#9508; Cell Signaling Technology), β-actin (#4967; Cell Signaling Technology), and PAR-1 (bs-0828R; Biosynthesis Biotechnology Co, Ltd, Beijing, China) at 4°C, followed by a horseradish peroxidase–linked secondary antibody for 2 h at room temperature. After development, membranes were stripped and reblotted with β-actin antibody. The immunoreactive bands were detected using the ImageQuant LAS 4000 mini system (GE Healthcare UK Ltd, Buckinghamshire, UK), and the intensities were then quantified using a densitometry tool (NIH

ImageJ software; https://imagej.nih.gov/ij/) and normalized to the internal control (β-actin protein).

Hepatic SECs and H/R models

Human hepatic SECs were purchased from ScienCell Research Laboratories (San Diego, CA). The H/R models were established using an AnaeroPack jar system (Mitsubishi Gas Chemical Co, Tokyo, Japan), as previously described.[36,37] In brief, SECs (1×10^6/well) were seeded and cultured in an endothelial cell medium (ScienCell Research Laboratories) on a 6-well collagen-coated plate at 37°C with 5% CO_2 for 24 h. After confluence, the cells cultured in serum-starved medium were exposed to hypoxic conditions (<0.1% O_2) for 12 h, followed by reoxygenation for 4 h.

Experimental groups of SECs

SECs were allocated to two H/R groups and two nonischemic control groups as follows and then cultured ($n = 5$ in each group). The H/R + vorapaxar group (H/R-1) was pretreated with 0.3 μM of vorapaxar in the endothelial cell medium for 2 h, whereas the H/R + vehicle group (H/R-2) was pretreated with vehicle (DMSO equivalent to that used to dissolve vorapaxar) for 2 h, followed by exposure to 12 h hypoxia and 4 h reoxygenation using an AnaeroPack jar system, respectively. The sham + vorapaxar group (nonischemic controls 1) was pretreated with 0.3 μM of vorapaxar in the endothelial cell medium for 2 h, whereas the sham + vehicle group (nonischemic controls 2) was pretreated with vehicle (DMSO equivalent to that used to dissolve vorapaxar) for 2 h, before incubation without hypoxia with the same timing as that of the H/R groups, respectively.

For the *in vitro* study under the inhibition of the ERK 1/2 signaling pathway using a specific MAPK inhibitor (PD98059; Sigma Aldrich, St. Louis, MO), SECs were preincubated with or without 10 μM of PD98059 for 2 h followed by treatment with or without 0.3 μM of vorapaxar. Subsequently, the cells were exposed to 12 h of hypoxia and 4 h of reoxygenation using the anaerobic jar system. Thereafter, the following four experimental groups were constructed *in vitro* ($n = 5$ in each group): (1) vehicle alone, (2) vorapaxar alone, (3) PD98059 + vorapaxar, and (4) PD98059 + vehicle.

Lactate dehydrogenase assay

Cell cytotoxicity was assessed by measuring lactate dehydrogenase (LDH) levels in the supernatant using a Cytotoxicity LDH Assay Kit-WST (Dojindo, Japan), following the manufacturer's instructions.

Data analysis

Data were expressed as medians and interquartile ranges. Differences between groups were analyzed using the Mann–Whitney *U*-test in SPSS (version 24; IBM Corp, Armonk, NY, USA). Multiple comparisons were performed using the Kruskal–Wallis test followed by the Mann–Whitney *U*-test with the Benjamini–Hochberg correction to control the false discovery rate at the 0.05 level using R (version 3.6.1; R Foundation for Statistical Computing, Vienna, Austria). $P < 0.05$ was considered statistically significant.

Results

PAR-1 was located on SECs and its expression was enhanced after hepatic IRI

Immunohistochemical analysis revealed that PAR-1 was located on SECs in both naïve livers (Fig. 1A-a) and livers after IRI (Fig. 1A-b). Immunofluorescent analysis showed coexpression of PAR-1 in green and cluster of differentiation 31 (CD31) in red, a major endothelial marker, in SECs in naïve livers (Fig. 1B) and livers after IRI (Fig. 1C). In addition, PAR-1 expression was significantly increased after IRI compared with the naïve group based on Western blot analysis (PAR-1/β-actin: 0.94 [0.88-1.08] in naïve, 4.20 [2.03-6.68] after IRI, $P = 0.01$; Figure 1D).

In Western blot analysis of SECs *in vitro*, PAR-1 expression was significantly increased after H/R compared with the naïve group (PAR-1/β-actin: 1.07 [0.57-1.18] in naïve, 3.41 [3.16-3.41] after H/R, $P = 0.009$; Figure 1E). LDH cytotoxicity levels in the supernatant of SEC cultures after H/R were significantly higher than those in the naïve group (0.89 [0.86-1.32] in naïve, 29.80 [26.18-29.80] after H/R, $P = 0.009$; Figure 1F).

The PAR-1 antagonist, vorapaxar, ameliorated hepatocellular injury

IRI livers treated with vehicle were characterized by sinusoidal vascular congestion (Fig. 2A-a), which was observed diffusely from the periportal area to the pericentral area, and congestion was, if anything, severe in the pericentral area. By contrast, IRI livers treated with vorapaxar showed suppressed congestion (Fig. 2A-b). Immunohistochemistry of Ly6G-positive cells, which are known as neutrophil-specific markers, demonstrated diffuse inflammatory infiltration in the IRI liver with vehicle (Fig. 2A-c) and vorapaxar (Fig. 2A-d). The modified Suzuki's score was significantly lower in the IRI + vorapaxar than in the IRI + vehicle group (6.5 [5.4-7.1] in IRI + vehicle, 2.8 [2.0-3.9] in IRI + vorapaxar, $P = 0.004$; Figure 2B). The number of Ly6G-positive cells was not significantly different between the IRI + vehicle and IRI + vorapaxar groups (12 [10-15] in IRI + vehicle, 10 [9-19] in IRI + vorapaxar, $P = 0.337$; Fig. 2C).

As shown in Figure 2D and E, vorapaxar significantly decreased serum AST and ALT levels compared with vehicle (AST: 3109 [2766-3665] IU/L in IRI + vehicle, 1808 [1593-2131] IU/L in IRI + vorapaxar, $P = 0.006$; ALT: 3629 [2180-4331] IU/L in IRI + vehicle, 1559 [1408-1837] IU/L in IRI + vorapaxar, $P = 0.025$).

Vorapaxar reduced apoptosis caused by hepatic IRI

Apoptosis of liver specimens after IRI was evaluated by TUNEL staining in the IRI + vehicle (Fig. 3A-a) and IRI + vorapaxar groups (Fig. 3A-b). Vorapaxar treatment markedly reduced the number of TUNEL-positive cells that appeared almost hepatocyte-like, compared with vehicle (135 [120-155] in

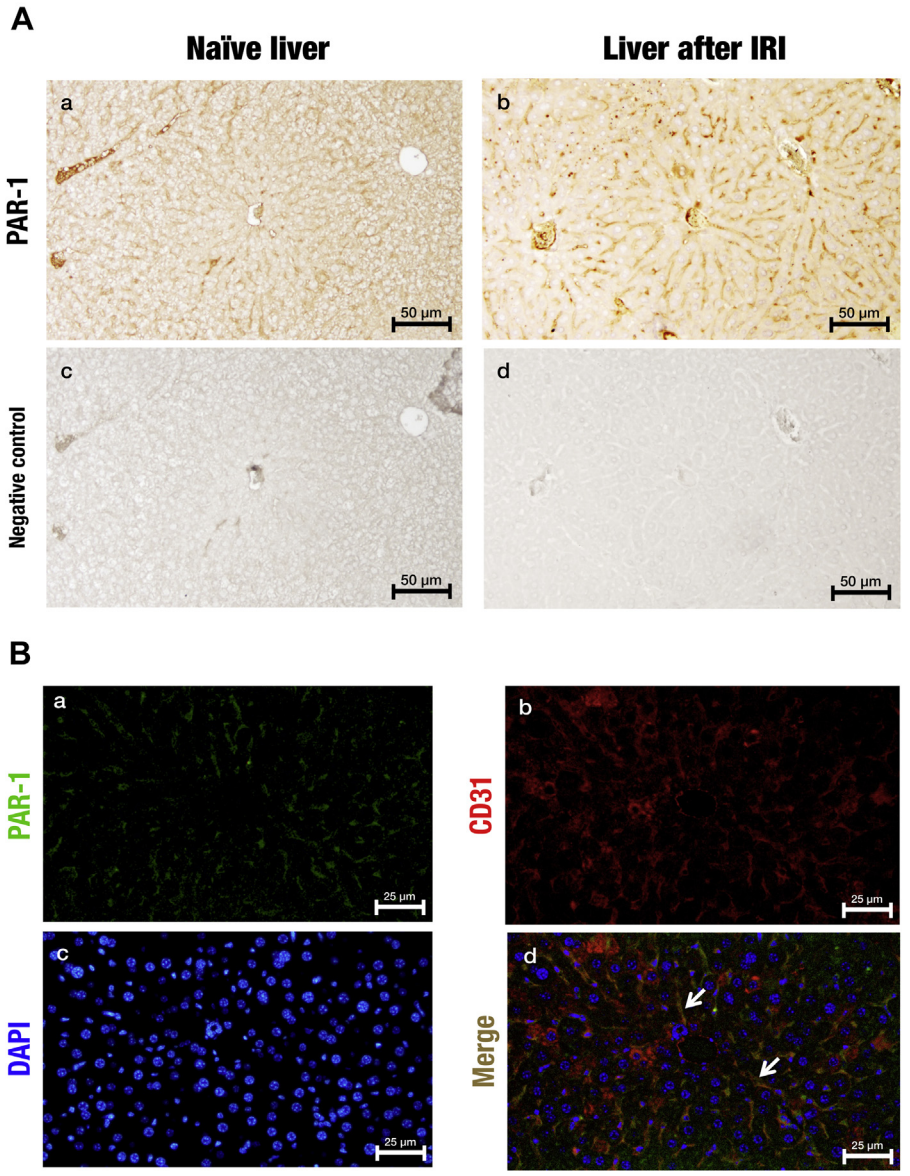

Fig. 1 – Characterization of PAR-1 expression in hepatic IRI models of mice and H/R models of hepatic SECs. (A) Immunohistochemical analysis revealed that PAR-1 was located on SECs in both naïve livers and livers after IRI (original magnification × 100). a: PAR-1 staining in naïve livers, b: PAR-1 staining in livers after IRI, c and d: negative controls. Immunofluorescence analysis revealed that PAR-1–positive staining was detected in SECs, as was CD31 (an endothelial marker)-positive staining, in both (B) naïve livers and (C) livers after IRI (original magnification × 100). a: PAR-1 in green, b: CD31 in red, c: DAPI (nuclear stain) in blue, d: merged image (arrows denote both PAR-1–positive and CD31-positive staining). (D) Western blot analysis showed that PAR-1 expression was significantly increased after IRI ($n = 6$ in each group). In an *in vitro* study, (E) PAR-1 expression in human hepatic SECs was significantly increased after H/R ($n = 5$ in each group), and (F) LDH cytotoxicity levels in the supernatant of SEC cultures after H/R were significantly higher than those in the naïve group ($n = 5$ in each group). Quantification of PAR-1 band intensities normalized to β-actin. H/R was established using an AnaeroPack jar system. (Color version of figure is available online.)

IRI + vehicle, 25 [11-34] in IRI + vorapaxar, $P = 0.004$; Figure 3B). In the IRI groups, vorapaxar treatment attenuated activation of caspase 9 compared with vehicle according to Western blot analysis (cleaved-caspase 9/pro-caspase 9: 0.96 [0.78-1.10] in IRI + vehicle, 0.36 [0.16-0.50] in IRI + vorapaxar, $P = 0.004$; Figure 3D). In nonischemic controls, no significant difference was found between treatment with vorapaxar and vehicle (cleaved-caspase 9/pro-caspase 9: 0.157 [0.153-0.185] in sham + vehicle, 0.145 [0.072-0.156] in sham + vorapaxar, $P = 0.297$; Figure 3C).

Vorapaxar-induced phosphorylation of AKT and ERK 1/2

To evaluate cell survival signaling, we examined the activation of AKT and ERK 1/2 in the liver. In the IRI groups, vorapaxar treatment markedly induced phosphorylation of both

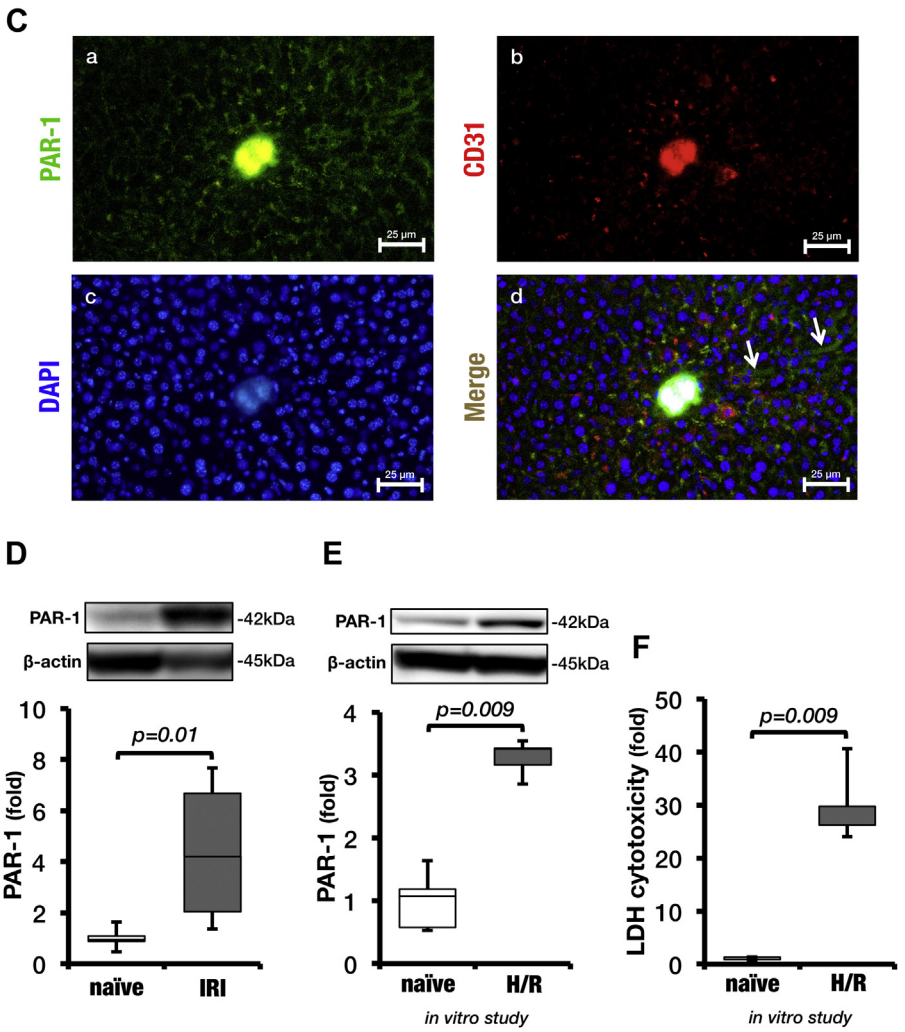

Fig. 1 – (*continued*).

AKT (phospho-AKT/total AKT: 1.06 [0.94-1.15] in IRI + vehicle, 2.92 [1.83-3.03] in IRI + vorapaxar, $P = 0.016$; Figure 3F) and ERK 1/2 (phospho-ERK/total ERK 1/2: 0.96 [0.89-1.02] in IRI + vehicle, 5.34 [2.71-7.66] in IRI + vorapaxar, $P = 0.004$; Figure 3H). In nonischemic controls, although no significant difference was seen in AKT phosphorylation between treatment with vorapaxar and vehicle (phospho-AKT/total AKT: 0.57 [0.54-0.65] in sham + vehicle, 0.57 [0.47-0.63] in sham + vorapaxar, $P = 0.749$; Figure 3E), vorapaxar treatment significantly mediated phosphorylation of ERK 1/2 compared with vehicle (phospho-ERK/total ERK 1/2: 0.37 [0.34-0.46] in sham + vehicle, 0.61 [0.54-0.78] in sham + vorapaxar, $P = 0.006$; Figure 3G).

Vorapaxar reduced apoptosis of SECs and induced phosphorylation of AKT and ERK 1/2 in vitro

Apoptotic cells were detected by TUNEL staining in the H/R + vehicle (Fig. 4A-a) and H/R + vorapaxar groups (Fig. 4A-b). Preincubation of SECs with vorapaxar markedly reduced the number of TUNEL-positive cells compared with vehicle (39.2 [27.4-49.3] in H/R + vehicle, 4.0 [3.5-4.9] in H/R + vorapaxar, $P = 0.021$; Figure 4B). According to the results of Western blot analysis, activation of caspase 9 was significantly attenuated in SECs pretreated with vorapaxar followed by exposure to H/R compared with vehicle (cleaved-caspase 9/pro-caspase 9: 1.14 [0.66-1.283] in H/R + vehicle, 0.41 [0.30-0.54] in H/R + vorapaxar, $P = 0.047$; Figure 4D). In nonischemic controls, no significant difference was seen in caspase 9 activation between pretreatment with vorapaxar and with vehicle (cleaved-caspase 9/pro-caspase 9: 0.105 [0.103-0.109] in sham + vehicle, 0.068 [0.065-0.082] in sham + vorapaxar, $P = 0.076$; Figure 4C). In the H/R groups, vorapaxar treatment markedly induced phosphorylation of both AKT (phospho-AKT/total AKT: 1.10 [0.81-1.15] in H/R + vehicle, 1.93 [1.49-2.10] in H/R + vorapaxar, $P = 0.047$; Figure 4F) and ERK 1/2 (phospho-ERK/total ERK 1/2: 0.66 [0.61-1.27] in H/R + vehicle, 3.04 [2.93-4.01] in H/R + vorapaxar, $P = 0.009$; Figure 4H). In nonischemic controls, no significant difference in AKT phosphorylation was found between vorapaxar and vehicle treatment (phospho-AKT/total AKT: 0.52 [0.49-0.53] in sham + vehicle, 0.54 [0.52-0.58] in sham + vorapaxar, $P = 0.347$; Figure 4E). Meanwhile, preincubation with vorapaxar significantly induced phosphorylation of ERK 1/2 compared with vehicle (phospho-ERK/total ERK 1/2: 0.13 [0.11-0.14] in sham + vehicle, 0.34 [0.29-0.35] in sham + vorapaxar,

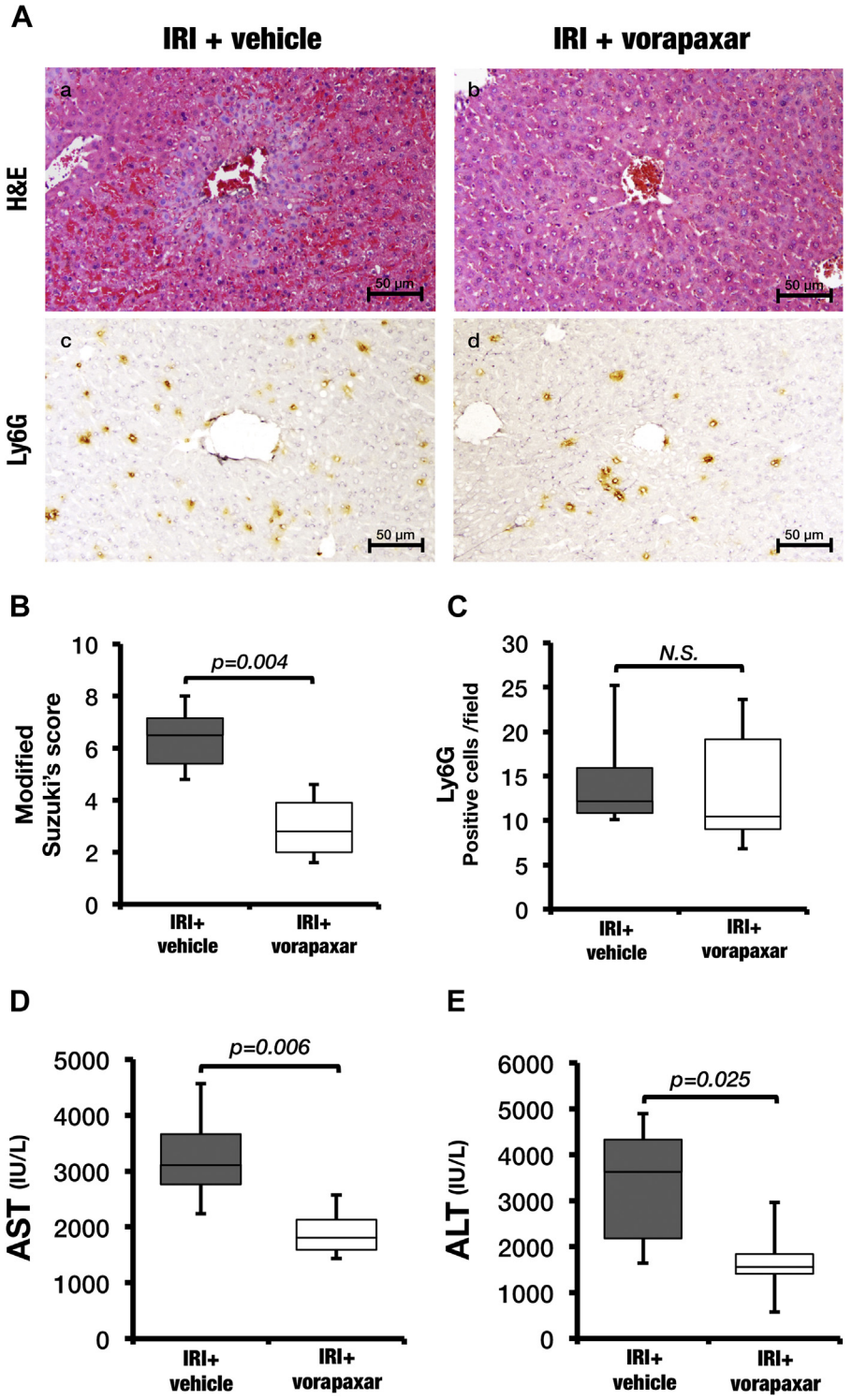

Fig. 2 – Liver histology and transaminases after hepatic IRI with or without vorapaxar. (A) IRI livers treated with (A) vehicle were characterized by sinusoidal vascular congestion, which was observed diffusely from the periportal area to the pericentral area, and congestion was, if anything, severe in the pericentral area. By contrast, IRI livers treated with (B) vorapaxar showed suppressed congestion (original magnification × 100). Immunohistochemistry of Ly6G-positive cells showed inflammatory infiltration in the IRI liver with (C) vehicle or (D) vorapaxar (original magnification × 100). (B) The modified Suzuki's score in the IRI + vorapaxar group was significantly lower than that in the IRI + vehicle group ($n = 6$ in each group). (D) The number of Ly6G-positive cells was not significantly different between the IRI + vehicle and IRI + vorapaxar groups ($n = 6$ in each group; $P = 0.337$). In the IRI groups, vorapaxar treatment significantly decreased serum levels of (D) AST and (E) ALT compared with vehicle ($n = 6$ in each group). (Color version of figure is available online.)

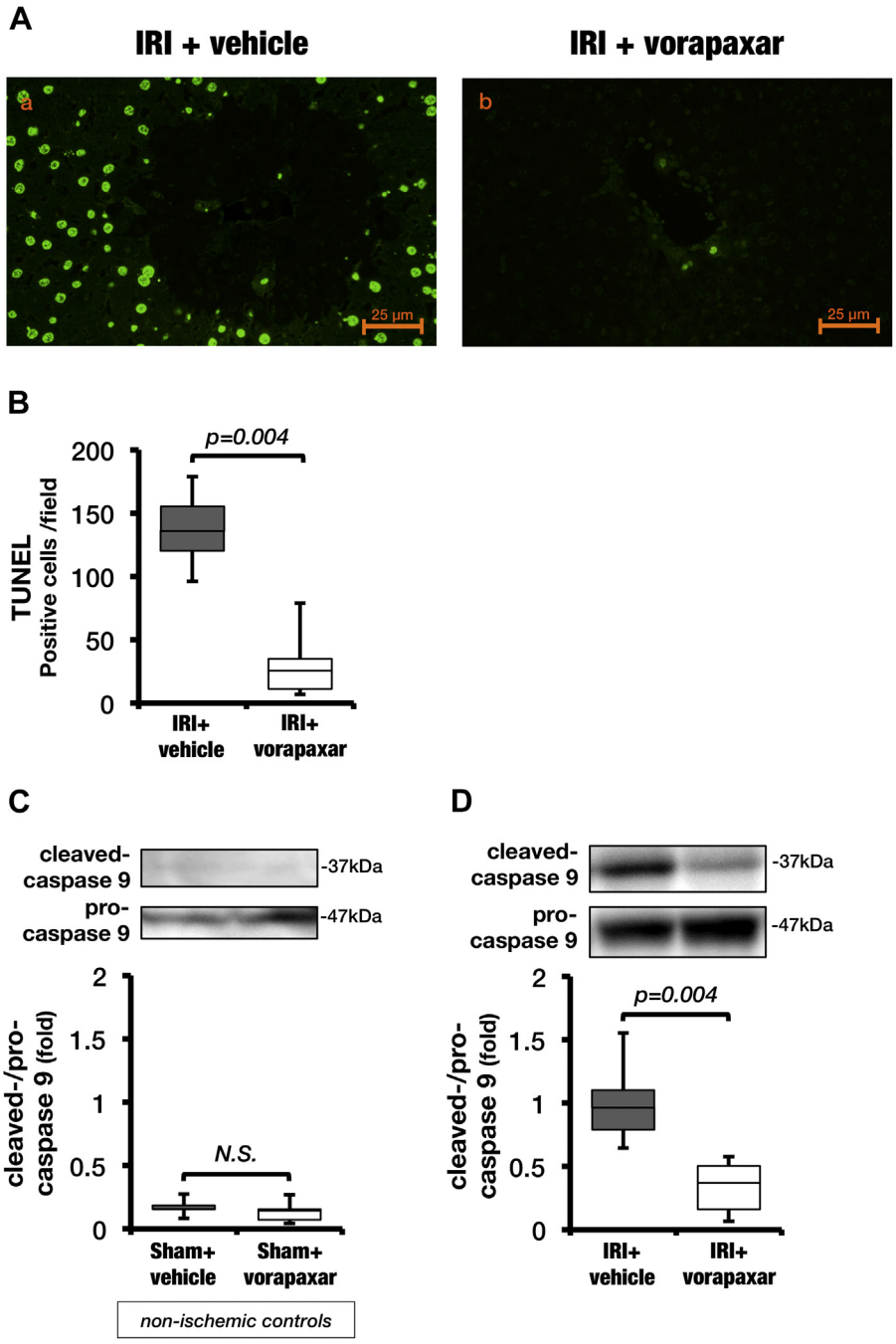

Fig. 3 – Antiapoptotic effect of vorapaxar and phosphorylation of AKT and ERK 1/2 induced by vorapaxar. (A) Apoptosis of liver specimens after IRI was evaluated by TUNEL staining in the (A) IRI + vehicle group and (B) IRI + vorapaxar group (original magnification × 200). (B) The average number of TUNEL-positive cells per field was significantly decreased by vorapaxar treatment compared with vehicle ($n = 6$ in each group). (C) In nonischemic controls, no significant difference was seen in caspase 9 activation between vorapaxar treatment and vehicle ($n = 6$ in each group; $P = 0.297$). (D) In the IRI groups, according to Western blot analysis, vorapaxar treatment reduced activation of caspase 9 compared with vehicle ($n = 6$ in each group). Quantification of cleaved-caspase 9 band intensities normalized to pro-caspase 9. (E) In nonischemic controls, no significant difference in AKT phosphorylation was seen between vorapaxar treatment and vehicle ($n = 6$ in each group; $P = 0.749$). (F) In the IRI groups, vorapaxar treatment markedly induced phosphorylation of AKT compared with vehicle ($n = 6$ in each group). In both the (G) nonischemic controls and (H) IRI groups, vorapaxar treatment markedly induced phosphorylation of ERK 1/2 compared with vehicle ($n = 6$ in each group). Quantification of phospho-AKT or ERK 1/2 band intensities normalized to total-AKT or ERK 1/2. (Color version of figure is available online.)

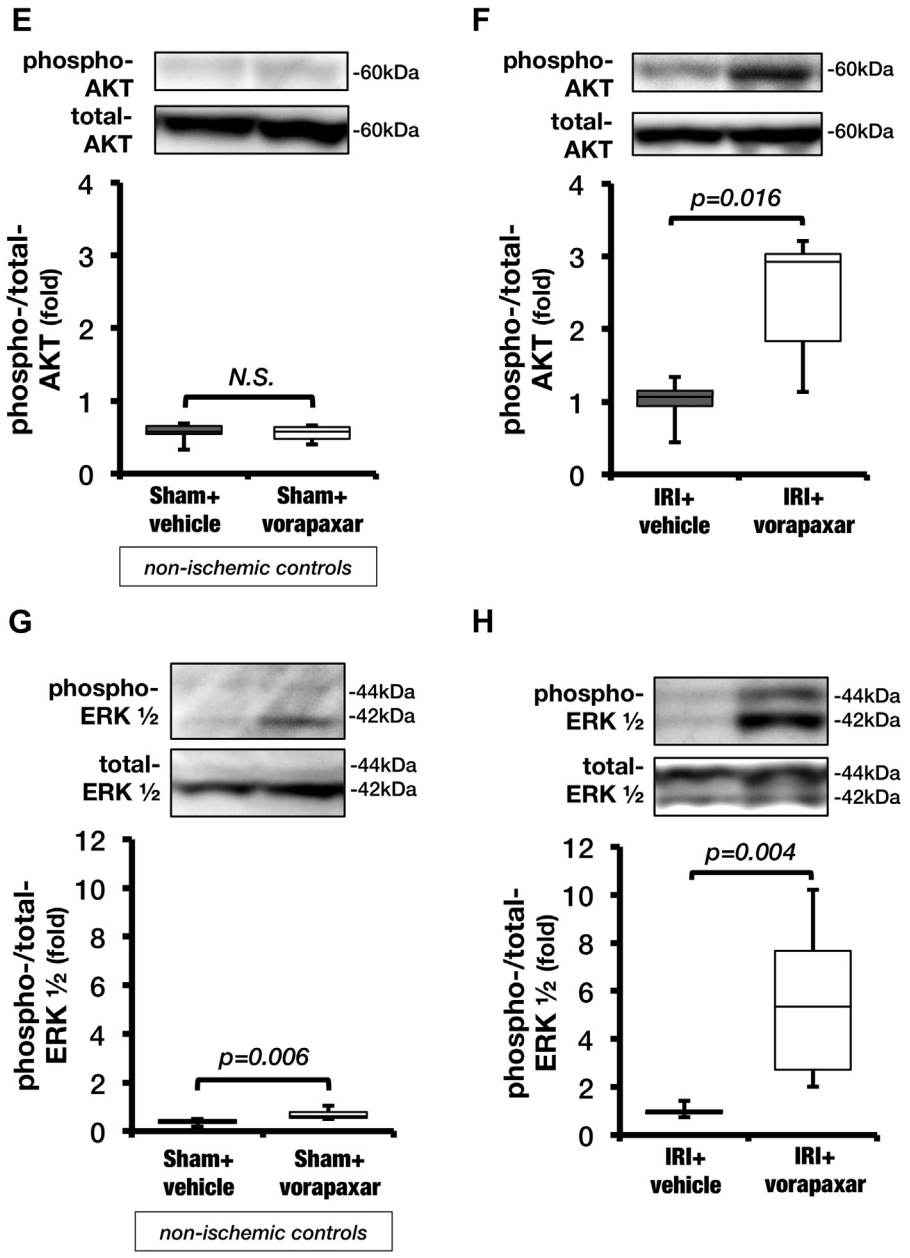

Fig. 3 – (*continued*).

$P = 0.009$; Figure 4G). In the H/R groups, LDH cytotoxicity levels in the supernatant of SEC cultures pretreated with vorapaxar were significantly lower compared with vehicle (0.98 [0.88-1.03] in H/R + vehicle, 0.74 [0.73-0.75] in H/R + vorapaxar, $P = 0.009$; Figure 4J), whereas pretreatment with vorapaxar in nonischemic controls did not reduce LDH cytotoxicity levels compared with vehicle (0.198 [0.194-0.237] in sham + vehicle, 0.208 [0.198-0.205] in sham + vorapaxar, $P = 1.0$; Figure 4I).

The inhibition of ERK 1/2 signaling pathway abolished the antiapoptotic effects of vorapaxar against H/R in vitro

The addition of pretreatment with PD98059, an inhibitor of the ERK 1/2 surviving signaling pathway, did not significantly increase LDH cytotoxicity levels in the SEC cultures improved by vorapaxar treatment compared with the vorapaxar alone and PD98059 + vorapaxar groups (0.56 [0.41-0.60] in vorapaxar alone, 0.68 [0.67-0.74] in PD98059 + vorapaxar, $P = 0.067$; Figure 5A).

As shown in Figure 5B, the addition of preincubation with PD98059 significantly activated caspase 9 compared with the vorapaxar alone and PD98059 + vorapaxar groups (cleaved-caspase 9/pro-caspase 9: 0.45 [0.34-0.51] in vorapaxar alone, 0.68 [0.60-0.74] in PD98059 + vorapaxar, $P = 0.016$). On the other hand, no significant difference was seen between the vehicle alone and PD98059 + vehicle groups (0.95 [0.74-1.07] in vehicle alone, 1.08 [0.85-1.10] in PD98059 + vehicle, $P = 0.548$). Furthermore, preincubation of SECs with PD98059 followed by vorapaxar treatment markedly reduced phosphorylation of ERK 1/2 mediated by vorapaxar treatment compared with the

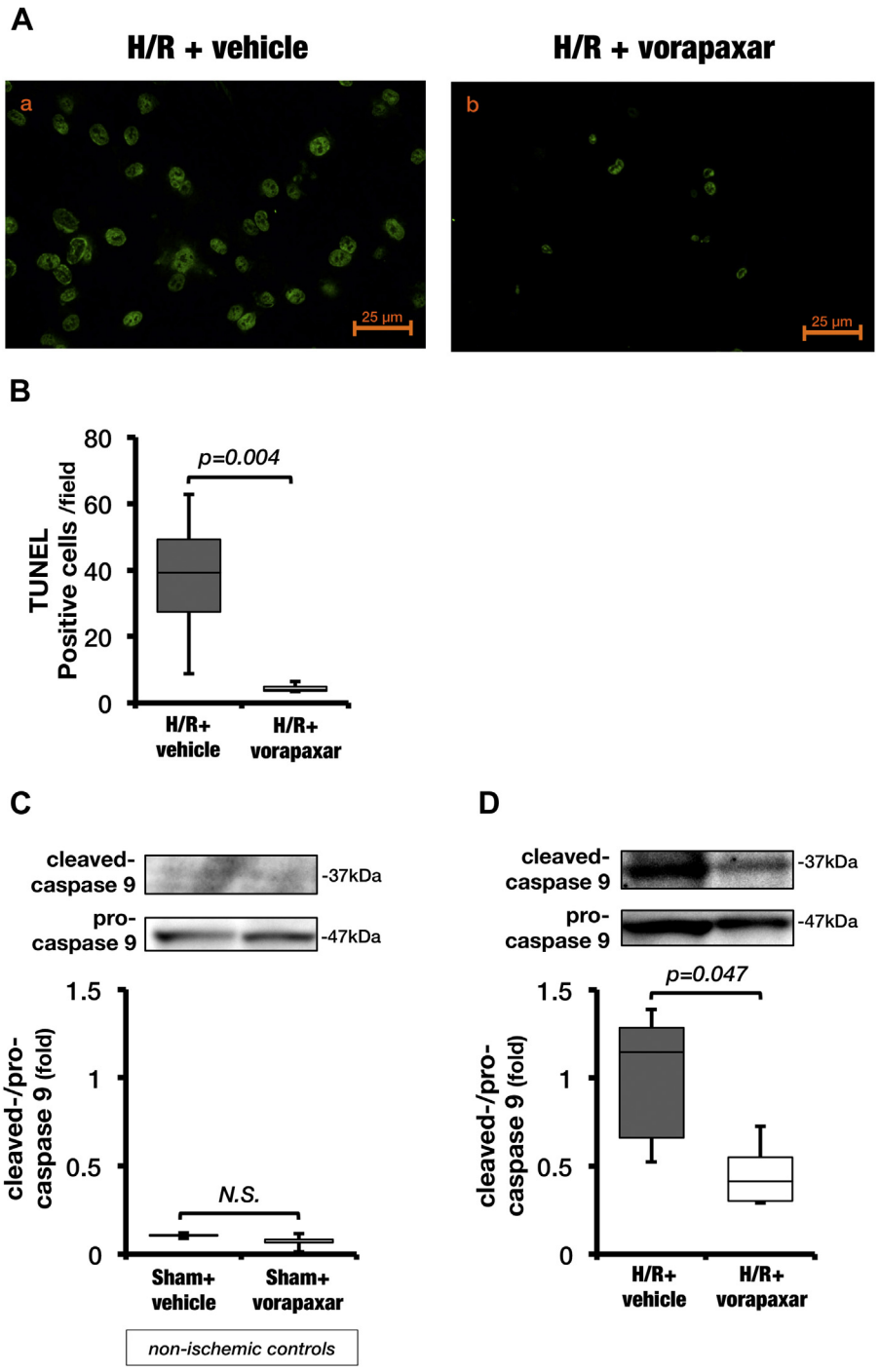

Fig. 4 – Direct effect of vorapaxar on hepatic SECs in in vitro H/R models. (A) Apoptotic cells were detected by TUNEL staining in the (A) H/R + vehicle and (B) H/R + vorapaxar groups (original magnification × 200). (B) The average number of TUNEL-positive cells per field was significantly decreased with vorapaxar treatment compared with vehicle ($n = 4$ in each group). (C) In nonischemic controls, no significant difference in caspase 9 activation was seen between vorapaxar treatment and vehicle ($n = 5$ in each group; $P = 0.076$). (D) In the H/R groups, based on Western blot analysis, vorapaxar treatment reduced activation of caspase 9 compared with vehicle ($n = 5$ in each group). Quantification of cleaved-caspase 9 band intensities normalized to procaspase 9. (E) In nonischemic controls, no significant difference in AKT phosphorylation was seen between pretreatment with vorapaxar and vehicle ($n = 5$ in each group; $P = 0.347$). (F) In the H/R groups, vorapaxar treatment markedly induced phosphorylation of AKT compared with vehicle ($n = 5$ in each group). In both the (G) nonischemic controls and (H) H/R group, vorapaxar treatment markedly induced phosphorylation of ERK 1/2 compared with vehicle ($n = 5$ in each group). Quantification of phospho-AKT or ERK 1/2 band intensities normalized to total-AKT or ERK 1/2. (I) In nonischemic controls, vorapaxar treatment did not reduce LDH cytotoxicity levels compared with vehicle ($n = 5$ in each group; $P = 1.0$), whereas (J) in the H/R groups ($n = 5$ in each group), vorapaxar treatment significantly reduced LDH cytotoxicity levels compared with vehicle. H/R was established using an AnaeroPack jar system. (Color version of figure is available online.)

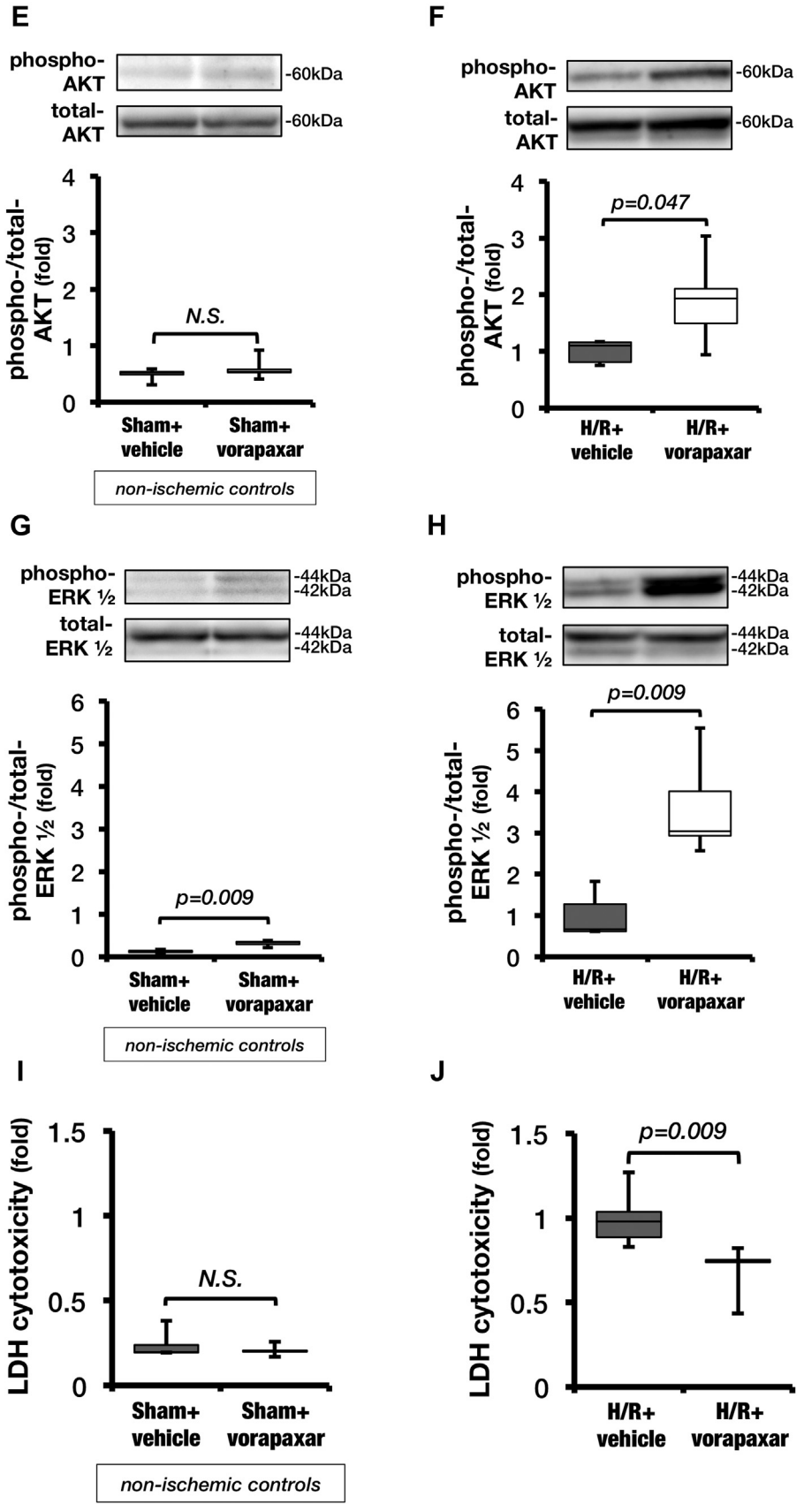

Fig. 4 – (*continued*).

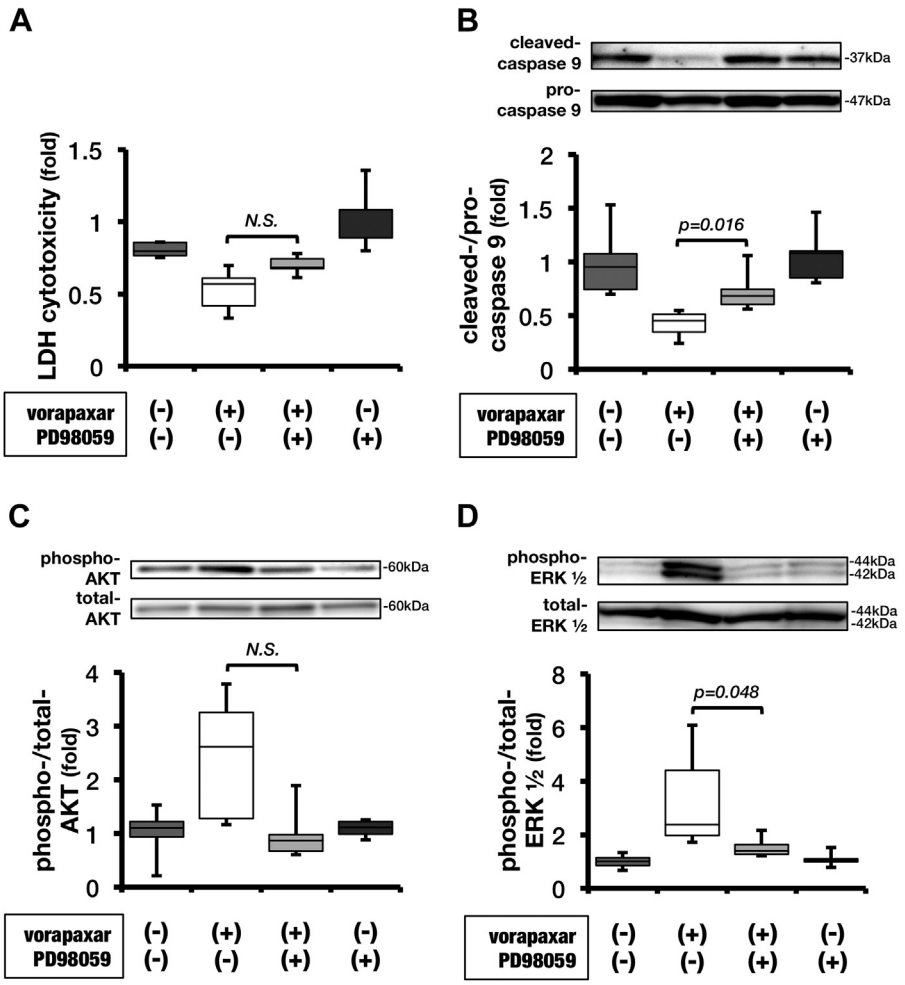

Fig. 5 – Mechanisms underlying the antiapoptotic effect of vorapaxar on hepatic SECs *in vitro*. (A) In a comparison between the vorapaxar alone and PD98059 + vorapaxar groups, the addition of pretreatment with PD98059, which is an inhibitor of the ERK 1/2 surviving signaling pathway, did not significantly increase LDH cytotoxicity levels in the supernatant of SEC cultures improved by vorapaxar treatment ($n = 5$ in each group; $P = 0.067$). Based on Western blot analysis, (B) the addition of pretreatment with PD98059 significantly increased activation of caspase 9 compared with the vorapaxar alone and PD98059 + vorapaxar groups ($n = 5$ in each group). In a comparison between the vorapaxar alone and PD98059 + vorapaxar groups, (C) the addition of pretreatment with PD98059 did not reduce phosphorylation of AKT ($n = 5$ in each group; $P = 0.095$); however, (D) phosphorylation of ERK 1/2 was markedly reduced by the addition of pretreatment with PD98059 ($n = 5$ in each group). Quantification of cleaved-caspase 9 band intensities normalized to procaspase 9. Quantification of phospho-AKT or ERK 1/2 band intensities normalized to total AKT or ERK 1/2. H/R was established using an AnaeroPack jar system.

vorapaxar alone and PD98059 + vorapaxar groups, whereas no significant difference was found between the vehicle alone and PD98059 + vehicle groups (phospho-ERK/total ERK 1/2: 2.38 [1.97-4.39] in vorapaxar alone, 1.39 [1.27-1.63] in PD98059 + vorapaxar, $P = 0.048$; and 1.00 [0.85-1.14] in vehicle alone, 1.03 [0.99-1.09] in PD98059 + vehicle, $P = 0.841$; Figure 5D). In contrast to the results of ERK 1/2, the addition of preincubation with PD98059 did not reduce AKT phosphorylation significantly compared with the vorapaxar alone and PD98059 + vorapaxar groups (phospho-AKT/total AKT: 2.61 [1.27-3.25] in vorapaxar alone, 0.86 [0.66-0.97] in PD98059 + vorapaxar, $P = 0.095$; Figure 5C).

Discussion

In the present study, PAR-1 was confirmed to be located on hepatic SECs by immunohistochemistry and immunofluorescence analysis. Our *in vivo* and *in vitro* studies revealed for the first time that IRI strongly enhanced PAR-1 expression on hepatic SECs. Highly selective PAR-1 antagonist (vorapaxar) treatment for hepatic IRI models of mice significantly decreased serum transaminase levels, improved liver histological damage, reduced the number of apoptotic cells, attenuated the activation of caspase 9, and activated cell

survival signaling based on the phosphorylation of AKT and ERK 1/2. Moreover, in an *in vitro* study using H/R models of pure cultured hepatic SECs, preincubation with vorapaxar also attenuated apoptosis and caspase 9 activation caused by H/R and induced phosphorylation of AKT and ERK 1/2, whereas the reduction in caspase 9 activation and phosphorylation of ERK 1/2 provided by vorapaxar were abolished by adding the inhibitor of the ERK 1/2 signaling pathway.

PAR-1 can be detected in various kinds of organs and blood cells,[38-40] and PAR-1 activation by thrombin contributes to tissue injury.[41] Regarding the human liver, in 1998, Marra *et al.*[42] investigated the expression of the thrombin receptor, which is now consistent with PAR-1, using immunohistochemistry and *in situ* hybridization. They found that the thrombin receptor was present in SECs in the normal liver and that its expression was markedly upregulated during fulminant hepatitis, with the highest expression in mesenchymal cells in areas of regeneration. Since the first report by Marra *et al.*, there have only been a few studies on PAR-1 expression in the liver.[42-44] To the best of our knowledge, the present study reveals for the first time that IRI strongly enhances PAR-1 expression in hepatic SECs. Because SECs are the initial target of hepatic IRI,[45,46] we hypothesized that SEC injury directly induces upregulation of PAR-1 expression. In agreement with this hypothesis, our *in vitro* study revealed that PAR-1 expression was upregulated by only H/R stress in pure cultured hepatic SECs. On the other hand, the mechanism of regulation of PAR-1 expression is not fully understood. Using a mouse model of bacterial pulmonary infection by *Streptococcus pneumoniae*, Jose *et al.*[31] demonstrated that alveolar endothelial cell injury caused by neutrophilic inflammation enhanced PAR-1 expression, and speculated that Rac-1, which is part of the Rho A family,[47] maintained PAR-1 surface expression. Because Rac-1 in the liver is involved in the capillary-like tube formation accompanying sinusoidal endothelial fenestrae contraction,[48] it might regulate PAR-1 expression in hepatic SECs. Further studies are needed to clarify the mechanism of PAR-1 regulation in SEC injury.

PAR-1 activation induced by thrombin elicits inflammation signaling through the upregulation of various inflammatory mediators, including tumor necrosis factor-α (TNF-α) and interleukin-6, and cell adhesion molecules, including intercellular adhesion molecule-1 and vascular cell adhesion molecule-1.[41] Moreover, PAR-1 activation induces apoptosis through the activation of caspase,[30,49] which plays a central role in the execution of apoptosis.[50] Considering these facts and our findings regarding the enhancement of PAR-1 expression during hepatic IRI, we hypothesized that the upregulation of PAR-1 induced by IRI further exacerbates liver injury, and accordingly, PAR-1 antagonism against hepatic IRI provides cytoprotective effects, which appear as the attenuation of inflammation or apoptosis. Indeed, the anti-inflammatory or antiapoptotic effects provided by PAR-1 antagonism have been reported in previous IRI studies. El Eter *et al.*[28] reported that blocking PAR-1 using SCH79797, a PAR1 antagonist for research use only, limited renal IRI via an anti-inflammatory effect, thereby inhibiting pivotal proinflammatory cytokines such as TNF-α and cytokine-induced neutrophil chemoattractant-1, which reflects leukocyte activation and inflammation. Rajput *et al.*[27] observed a significantly reduced number of TUNEL positive cells in PAR-1 knockdown rats in cerebral IRI models. However, to our knowledge, no reports have described a study of hepatic IRI investigating PAR-1 antagonism. In the present hepatic IRI models of mice, we demonstrated that vorapaxar, a potent and selective PAR-1 antagonist, greatly improved liver histological damage and markedly attenuated apoptosis through the reduction of caspase 9 activation, which is promoted by the release of cytochrome c from the intermembrane space of mitochondria into the cytosol and leads to cell death via activating effector caspase 3 and 7.[51] By contrast, vorapaxar treatment did not prevent neutrophilic recruitment to the liver (Fig. 2A-c and -d) or reduce the generation of inflammatory cytokines such as TNF-α and interleukin-6 (data not shown). To the best of our knowledge, these findings represent the first *in vivo* evidence revealing the cytoprotective effects of a PAR-1 antagonist against hepatic IRI. Furthermore, regarding vorapaxar, there have been only two studies reporting cytoprotective effects, both of which showed only suppression of the inflammatory response; our study is thus also the first to describe an antiapoptotic effect.[31,52]

In addition, in the present *in vitro* study, we confirmed the direct effects of vorapaxar treatment on pure cultured hepatic SECs using H/R models because PAR-1 is also expressed in monocytes and lymphocytes recruited to the liver.[43] A few *in vitro* studies have examined the direct effects provided by PAR-1 antagonists on endothelial cells. Kim *et al.*[52] found that PAR-1 antagonists prevented inflammation via upregulation of zonula occludens-1, a tight-junction protein, in vascular endothelial cells. In the present study, we demonstrated that pretreatment with vorapaxar significantly decreased LDH cytotoxicity levels and prevented hepatic SECs from apoptosis caused by H/R injury through a reduction of caspase 9 activation and the number of TUNEL-positive cells. These findings are similar to those in our *in vivo* study using hepatic IRI models. Regarding hepatocytes, the present study revealed that PAR-1 was not located on hepatocytes, which was the same result as that in a previous report by Rullier *et al.*[43]; hence, we considered that vorapaxar treatment does not work on hepatocytes directly, and ascertained that preincubation of primary cultured hepatocytes with vorapaxar does not reduce apoptosis caused by H/R (Supplemental Fig. 2). However, the TUNEL-positive cells in our *in vivo* study appeared almost hepatocyte-like, and vorapaxar treatment also protected hepatocytes from apoptosis. These findings suggest that the protection of SECs by vorapaxar itself contributed to the survival of hepatocytes against apoptosis. In agreement with this hypothesis, Nowatari *et al.*[53] demonstrated that, using *in vitro* apoptotic models with staurosporine, a reagent that promotes intracellular stress, the survival of SECs promoted the proliferation of hepatocytes through the signal transducer and activator of the transcription 3 pathway in a paracrine manner. Consequently, we suggested that hepatic SECs are potentially dominant targets for PAR-1 antagonism with vorapaxar, and that vorapaxar provides direct cytoprotective effects on hepatic SECs, but not on hepatocytes. However, the precise mechanism of interaction between SECs and hepatocytes under vorapaxar treatment remains unclear, and thus, the further studies are required.

In addition, in the present *in vivo* and vitro studies, we revealed that vorapaxar treatment markedly activated cell survival signaling, such as AKT and ERK 1/2. AKT, one of the key signaling enzymes implicated in cell survival, can suppress cell death via inhibiting caspases and cellular inflammation via inhibition of NF-κB activation.[54,55] ERK 1/2 possesses direct antiapoptotic effects by downregulating proapoptotic molecules (BAD, Bim, Bax) and upregulating antiapoptotic molecules (Mcl-1, Bcl-2, Bcl-XL).[56-58] Although a lot of evidence indicates that both of these types of signaling play an important protective role in attenuating apoptosis, the relationship between the antiapoptotic effect conferred by PAR-1 antagonism and AKT or ERK 1/2 signaling remains unclear. However, regarding IRI studies, two previous reports proposed some findings demonstrating this relationship. Strande *et al.*[29] showed that AKT activation mediated by PAR-1 antagonism resulted in a decrease in apoptosis caused by myocardial IRI. Yang *et al.*[59] demonstrated that in cerebral IRI models of rabbits, treatment involving PAR-1 antagonism increased phosphorylated ERK 1/2 levels and attenuated effector caspase 3 activation. Accordingly, we focused on AKT and ERK 1/2 as downstream signaling mediated by the antiapoptotic effects of vorapaxar, which attenuated the activation of caspase 9. Thomas *et al.*[60] revealed that the activation of ERK 1/2, but not AKT, signaling was required for cardioprotective effects conferred by the reperfusion injury salvage kinase pathway in myocardial IRI, which consists of prosurvival and antiapoptotic mediators; this had previously been identified by Hausenloy.[61] Thomas *et al.*[60] used the phosphatidylinositol-3-OH kinase inhibitor, LY294002, which inhibited the upstream activators of AKT signaling, and the MAPK inhibitor, PD98059, which inhibited the upstream activators of ERK 1/2 signaling, in demonstrating that the inhibition of ERK 1/2 signaling by PD98059 blocked the reperfusion injury salvage kinase pathway, whereas the inhibition of AKT signaling by LY294002 had no effect. In addition to their results, our *in vivo* and vitro results of nonischemic controls demonstrated that vorapaxar treatment also activated ERK 1/2 in sham mice and SECs. Therefore, we first paid attention to ERK 1/2 rather than AKT and hypothesized that ERK 1/2 signaling was imperative for vorapaxar to exert its antiapoptotic effects sufficiently. In the present *in vitro* study using H/R models of SECs, we demonstrated that preincubation with PD98059, which led to the inhibition of ERK 1/2 signaling, abolished not only the phosphorylation of ERK 1/2 but also the attenuation of caspase 9 activation, both of which are beneficial effects induced by vorapaxar. According to Allan *et al.*,[62] caspase 9 activation mediated by the addition of cytochrome c was enhanced under the inhibition of ERK 1/2 by PD98059. By contrast, the inhibition of AKT by LY294002 had no effect on this activation. This finding also highlights the importance of ERK 1/2 signaling in terms of the mechanism of caspase 9 that regulates apoptotic cascades. Consequently, we concluded that the activation of ERK 1/2 signaling induced by vorapaxar treatment brought about a reduction in caspase 9 activation, resulting in the attenuation of apoptosis during hepatic IRI.

The present study also showed that AKT was activated by vorapaxar treatment; however, the interaction between the AKT and ERK 1/2 pathways remains to be clarified. In general, AKT and ERK 1/2 have been considered to be two parallel signaling pathways.[63,64] Recently, using brain IRI models, Zhou *et al.*[64] demonstrated crosstalk between AKT and ERK 1/2 depending on Ras-Raf signaling. Furthermore, Wang *et al.*[65] indicated that PAR-1–induced signal transduction was involved in the linkage between AKT and ERK 1/2 via Ras-Raf signaling. In the present study, the inhibition of ERK 1/2 signaling did not significantly reduce the AKT phosphorylation provided by vorapaxar. Further studies investigating whether the inhibition of AKT or Ras-Raf signaling can affect ERK 1/2 phosphorylation may help our understanding of the interaction between these signaling pathways.

In our treatment regimen for the IRI mice models, vorapaxar was administered twice, at 60 min before ischemia and immediately after reperfusion. We considered that administration twice, before, and after IRI was required to obtain a sufficient protective effect on hepatic IRI. According to the pharmacokinetic data of this drug, after oral administration, the maximum drug concentration time (T_{max}) is about 3 h in rats and 1 h in monkeys, and the elimination half-life ($T_{1/2}$) is 5 h in rats and 13 h in monkeys; however, there were no data for mice.[32] Our treatment regimen was determined based on these data. Mice were administered vorapaxar intraperitoneally to obtain a certain bioabsorption; therefore, it was expected that T_{max} and $T_{1/2}$ were much shorter compared with oral administration, so we considered that additional administration was required after IRI to maintain sufficient blood concentration. In the clinical setting, because the datasheet for this drug in humans shows that the blood concentration of vorapaxar may be sufficiently maintained during hepatic IRI with single oral administration (T_{max}: 1 h, $T_{1/2}$: 3 d), we consider that a single oral administration of vorapaxar several hours before general anesthesia may attenuate the liver damage caused by IRI in cases of major hepatectomy and liver transplantation. On the other hand, because vorapaxar is an antiplatelet agent, and its long-term administration increases the risk of bleeding,[66] it should be used carefully during the perioperative period. In the TRA 2°P-TIMI 50 trial,[67] however, the patients who continued therapy with vorapaxar while undergoing coronary artery bypass grafting did not show an increased risk of major bleeding compared with placebo.

In conclusion, hepatic IRI induces significant enhancement of PAR-1 expression on SECs, which may be associated with the suppression of survival signaling pathways such as ERK 1/2, resulting in severe apoptosis-induced hepatic damage. In this situation, vorapaxar, a selective PAR-1 antagonist, attenuates hepatic IRI via antiapoptotic effects by the activation of survival signaling pathways.

Acknowledgment

This work was supported by JSPS KAKENHI Grant No. JP16K10569.

Authors' contributions: D.N. and N.K. designed the study, performed the experiments and interpreted the data, and wrote the initial draft of the manuscript. T.I., T.F., and H.K. supported the first and corresponding authors in performing

the experiments. All other authors contributed to the data analysis and critically reviewed the study design and manuscript. All authors approved the final version of the manuscript and agree to be accountable for all aspects of the work in ensuring that questions related to the accuracy or integrity of any part of the work are appropriately investigated and resolved.

Disclosure

The authors report no proprietary or commercial interest in any product mentioned or concept discussed in this article.

Supplementary data

Supplementary data to this article can be found online at https://doi.org/10.1016/j.jss.2019.09.044.

REFERENCES

1. Zhai Y, Busuttil RW, Kupiec-Weglinski JW. Liver ischemia and reperfusion injury: new Insights into mechanisms of innate-adaptive immune-mediated tissue inflammation. *Am J Transplant*. 2011;11:1563–1569.
2. Fondevila C, Busuttil RW, Kupiec-Weglinski JW. Hepatic ischemia/reperfusion injury—a fresh look. *Exp Mol Pathol*. 2003;74:86–93.
3. Selzner N. Protective strategies against ischemic injury of the liver. *Gastroenterology*. 2003;125:917–936.
4. Lisman T, Porte RJ. Rebalanced hemostasis in patients with liver disease: evidence and clinical consequences. *Blood*. 2010;116:878–885.
5. Kloek J, Heger M, Gaag NVD, et al. Effect of preoperative biliary drainage on coagulation and fibrinolysis in severe obstructive cholestasis. *J Clin Gastroenterol*. 2010;44:646–652.
6. Kassel KM, Owens AP, Rockwell CE, et al. Protease-activated receptor 1 and hematopoietic cell tissue factor are required for hepatic steatosis in mice fed a western diet. *Ajpa*. 2011;179:2278–2289.
7. Owens III AP, Passam FH, Antoniak S, et al. Monocyte tissue factor–dependent activation of coagulation in hypercholesterolemic mice and monkeys is inhibited by simvastatin. *J Clin Invest*. 2012;122:558–568.
8. Coughlin SR. Protease-activated receptors in hemostasis, thrombosis and vascular biology. *J Thromb Haemost*. 2005;3:1800–1814.
9. Kassel KM, Sullivan BP, Cui W, Copple BL, Luyendyk JP. Therapeutic administration of the direct thrombin inhibitor argatroban reduces hepatic inflammation in mice with established fatty liver disease. *Ajpa*. 2012;181:1287–1295.
10. Kopec AK, Joshi N, Towery KL, et al. Thrombin inhibition with dabigatran protects against high-fat diet-induced fatty liver disease in mice. *J Pharmacol Exp Ther*. 2014;351:288–297.
11. Luyendyk JP, Sullivan BP, Guo GL, Wang R. Tissue factor-deficiency and protease activated receptor-1-deficiency reduce inflammation elicited by diet-induced steatohepatitis in mice. *Ajpa*. 2010;176:177–186.
12. Vu TK, Hung DT, Wheaton VI, Coughlin SR. Molecular cloning of a functional thrombin receptor reveals a novel proteolytic mechanism of receptor activation. *Cell*. 1991;64:1057–1068.
13. Charles TE. The protein C pathway. *Chest*. 2003;124:26S–32S.
14. McLaughlin JN, Shen L, Holinstat M, Brooks JD, DiBenedetto E, Hamm HE. Functional selectivity of G protein signaling by agonist peptides and thrombin for the protease-activated receptor-1. *J Biol Chem*. 2005;280:25048–25059.
15. Ossovskaya VS, Bunnett NW. Protease-activated receptors: contribution to physiology and disease. *Physiol Rev*. 2004;84:579–621.
16. Kaplanski G, Marin V, Fabrigoule M, et al. Thrombin-activated human endothelial cells support monocyte adhesion in vitro following expression of intercellular adhesion molecule-1 (ICAM-1; CD54) and vascular cell adhesion molecule-1 (VCAM-1; CD106). *Blood*. 1998;92:1259–1267.
17. Mosnier LO, Sinha RK, Burnier L, Bouwens EA, Griffin JH. Biased agonism of protease-activated receptor 1 by activated protein C caused by noncanonical cleavage at Arg46. *Blood*. 2012;120:5237–5246.
18. Finigan JH, Dudek SM, Singleton PA, et al. Activated protein C mediates novel lung endothelial barrier enhancement. *J Biol Chem*. 2005;280:17286–17293.
19. Joyce DE, Gelbert L, Ciaccia A, DeHoff B, Grinnell BW. Gene expression profile of antithrombotic protein c defines new mechanisms modulating inflammation and apoptosis. *J Biol Chem*. 2001;276:11199–11203.
20. Kuriyama N, Isaji S, Hamada T, et al. The cytoprotective effects of addition of activated protein C into preservation solution on small-for-size grafts in rats. *Liver Transpl*. 2010;16:1–11.
21. Matsuda A, Kuriyama N, Kato H, et al. Research article comparative study on the cytoprotective effects of activated protein C treatment in nonsteatotic and steatotic livers under ischemia-reperfusion injury. *Biomed Res Int*. 2015;2015:1–13.
22. Ito T, Kuriyama N, Kato H, et al. Sinusoidal protection by sphingosine-1-phosphate receptor 1 agonist in liver ischemia-reperfusion injury. *J Surg Res*. 2018;222:139–152.
23. Feistritzer C. Endothelial barrier protection by activated protein C through PAR1-dependent sphingosine 1-phosphate receptor-1 crossactivation. *Blood*. 2005;105:3178–3184.
24. Ludeman MJ, Kataoka H, Srinivasan Y, Esmon NL, Esmon CT, Coughlin SR. PAR1 cleavage and signaling in response to activated protein C and thrombin. *J Biol Chem*. 2005;280:13122–13128.
25. White LE, Hassoun HT. Inflammatory mechanisms of organ crosstalk during ischemic acute kidney injury. *Int J Nephrol*. 2012;2012:505197.
26. Chong AJ, Pohlman TH, Hampton CR, Shimamoto A, Mackman N, Verrier ED. Tissue factor and thrombin mediate myocardial ischemia-reperfusion injury. *Ann Thorac Surg*. 2003;75:S649–S655.
27. Rajput PS, Lyden PD, Chen B, et al. Protease activated receptor-1 mediates cytotoxicity during ischemia using in vivo and in vitro models. *Neuroscience*. 2014;281:229–240.
28. Eter El EA, Aldrees A. Inhibition of proinflammatory cytokines by SCH79797, a selective protease-activated receptor 1 antagonist, protects rat kidney against ischemia-reperfusion injury. *Shock*. 2012;37:639–644.
29. Strande JL, Hsu A, Su J, Fu X, Gross GJ, Baker JE. SCH 79797, a selective PAR1 antagonist, limits myocardial ischemia/reperfusion injury in rat hearts. *Basic Res Cardiol*. 2007;102:350–358.
30. Wang J, Jin H, Hua Y, Keep RF, Xi G. Role of protease-activated receptor-1 in brain injury after experimental global cerebral ischemia. *Stroke*. 2012;43:2476–2482.
31. José RJ, Williams AE, Mercer PF, Sulikowski MG, Brown JS, Chambers RC. Regulation of neutrophilic inflammation by proteinase-activated receptor 1 during bacterial pulmonary infection. *J Immunol*. 2015;194:6024–6034.
32. Chackalamannil S, Wang Y, Greenlee WJ, et al. Discovery of a novel, orally active himbacine-based thrombin receptor

antagonist (SCH 530348) with potent antiplatelet activity. *J Med Chem*. 2008;51:3061–3064.
33. Hamada T, Fondevila C, Busuttil RW, Coito AJ. Metalloproteinase-9 deficiency protects against hepatic ischemia/reperfusion injury. *Hepatology*. 2007;47:186–198.
34. Suzuki S, Toledo-Pereyra LH, Rodriguez FJ, Cejalvo D. Neutrophil infiltration as an important factor in liver ischemia and reperfusion injury. Modulating effects of FK506 and cyclosporine. *Transplantation*. 1993;55:1265–1272.
35. Duarte S, Hamada T, Kuriyama N, Busuttil RW, Coito AJ. TIMP-1 deficiency leads to lethal partial hepatic ischemia and reperfusion injury. *Hepatology*. 2012;56:1074–1085.
36. Wei R, Zhang R, Xie Y, Shen L, Chen F. Hydrogen suppresses hypoxia/reoxygenation-induced cell death in hippocampal neurons through reducing oxidative stress. *Cell Physiol Biochem*. 2015;36:585–598.
37. Xie F, Li Z-P, Wang H-W, et al. Evaluation of liver ischemia-reperfusion injury in rabbits using a nanoscale ultrasound contrast agent targeting ICAM-1. *PLoS One*. 2016;11:e0153805.
38. Macfarlane SR, Seatter MJ, Kanke T, Hunter GD, Plevin R. Proteinase-activated receptors. *Pharmacol Rev*. 2001;53:245–282.
39. Vergnolle N. Modulation of visceral pain and inflammation by protease-activated receptors. *Br J Pharmacol*. 2004;141:1264–1274.
40. Tsuboi H, Naito Y, Katada K, et al. Role of the thrombin/protease-activated receptor 1 pathway in intestinal ischemia-reperfusion injury in rats. *Am J Physiol Gastrointest Liver Physiol*. 2007;292:G678–G683.
41. Rezaie A. Protease-activated receptor signalling by coagulation proteases in endothelial cells. *Thromb Haemost*. 2017;112:876–882.
42. Marra F, DeFranco R, Grappone C, et al. Expression of the thrombin receptor in human liver: up-regulation during acute and chronic injury. *Hepatology*. 1998;27:462–471.
43. Rullier A, Senant N, Kisiel W, et al. Expression of protease-activated receptors and tissue factor in human liver. *Virchows Arch*. 2005;448:46–51.
44. Dupuy E, Hainaud P, Villemain A, et al. Tumoral angiogenesis and tissue factor expression during hepatocellular carcinoma progression in a transgenic mouse model. *J Hepatol*. 2003;38:793–802.
45. Kohli V, Selzner M, Madden JF, Bentley RC, Clavien P-A. Endothelial cell and hepatocyte deaths occur by apoptosis after ischemia-reperfusion injury in the rat liver. *Transplantation*. 1999;67:1099–1105.
46. Natori S, Selzner M, Valentino KL, et al. Apoptosis of sinusoidal endothelial cells occurs during liver preservation injury by a caspase-dependent mechanism. *Transplantation*. 1999;68:89–96.
47. Yufu T, Hirano K, Bi D, et al. Rac1 regulation of surface expression of protease-activated receptor-1 and responsiveness to thrombin in vascular smooth muscle cells. *Arterioscler Thromb Vasc Biol*. 2005;25:1506–1511.
48. Yokomori H, Oda M, Yoshimura K, et al. Caveolin-1 and rac regulate endothelial capillary-like tubular formation and fenestral contraction in sinusoidal endothelial cells. *Liver Int*. 2009;29:266–276.
49. Flynn AN, Buret AG. Proteinase-activated receptor 1 (PAR-1) and cell apoptosis. *Apoptosis*. 2004;9:729–737.
50. Budihardjo I, Oliver H, Lutter M, Luo X, Wang X. Biochemical pathways of caspase activation during apoptosis. *Annu Rev Cell Dev Biol*. 1999;15:269–290.
51. Salvesen GS, Abrams JM. Caspase activation – stepping on the gas or releasing the brakes? Lessons from humans and flies. *Oncogene*. 2004;23:2774–2784.
52. Kim HN, Kim YR, Ahn SM, Lee SK, Shin HK, Choi BT. Protease activated receptor-1 antagonist ameliorates the clinical symptoms of experimental autoimmune encephalomyelitis via inhibiting breakdown of blood-brain barrier. *J Neurochem*. 2015;135:577–588.
53. Nowatari T, Murata S, Nakayama K, et al. Sphingosine 1-phosphate has anti-apoptotic effect on liver sinusoidal endothelial cells and proliferative effect on hepatocytes in a paracrine manner in human. *Hepatol Res*. 2014;45:1136–1145.
54. Cantley LC. The phosphoinositide 3-kinase pathway. *Science*. 2002;296:1655–1657.
55. Zhang R, Zhang L, Manaenko A, Ye Z, Liu W, Sun X. Helium preconditioning protects mouse liver against ischemia and reperfusion injury through the PI3K/Akt pathway. *J Hepatol*. 2014;61:1048–1055.
56. Lu Z, Xu S. ERK1/2 MAP kinases in cell survival and apoptosis. *IUBMB Life*. 2006;58:621–631.
57. Yang J-Y, Michod D, Walicki J, Widmann C. Surviving the kiss of death. *Biochem Pharmacol*. 2004;68:1027–1031.
58. Perkins D, Pereira EFR, Aurelian L. The herpes simplex virus type 2 R1 protein kinase (ICP10 PK) functions as a dominant regulator of apoptosis in hippocampal neurons involving activation of the ERK survival pathway and upregulation of the antiapoptotic protein Bag-1. *J Virol*. 2003;77:1292–1305.
59. Yang J-N, Chen J, Xiao M. A protease-activated receptor 1 antagonist protects against global cerebral ischemia/reperfusion injury after asphyxial cardiac arrest in rabbits. *Neural Regen Res*. 2017;12:242–248.
60. Thomas CJ, Lim NR, Kedikaetswe A, et al. Evidence that the MEK/ERK but not the PI3K/Akt pathway is required for protection from myocardial ischemia–reperfusion injury by 3′,4′-dihydroxyflavonol. *Eur J Pharmacol*. 2015;758:53–59.
61. Hausenloy DJ, Yellon DM. Reperfusion injury salvage kinase signalling: taking a RISK for cardioprotection. *Heart Fail Rev*. 2007;12:217–234.
62. Allan LA, Morrice N, Brady S, Magee G, Pathak S, Clarke PR. Inhibition of caspase-9 through phosphorylation at Thr 125 by ERK MAPK. *Nat Cell Biol*. 2003;5:647–654.
63. Segarra J, Balenci L, Drenth T, Maina F, Lamballe F. Combined signaling through ERK, PI3K/AKT, and RAC1/p38 is required for met-triggered cortical neuron migration. *J Biol Chem*. 2006;281:4771–4778.
64. Zhou J, Du T, Li B, Rong Y, Verkhratsky A, Peng L. Crosstalk between MAPK/ERK and PI3K/AKT signal pathways during brain ischemia/reperfusion. *ASN Neuro*. 2015;7, 175909141560246.
65. Wang H, Ubl JJ, Stricker R, Reiser G. Thrombin (PAR-1)-induced proliferation in astrocytes via MAPK involves multiple signaling pathways. *Am J Physiol Cell Physiol*. 2002;283:C1351–C1364.
66. Morrow DA, Braunwald E, Bonaca MP, et al. Vorapaxar in the secondary prevention of atherothrombotic events. *N Engl J Med*. 2012;366:1404–1413.
67. David AM, Benjamin MS, Keith AAF, et al. Evaluation of a novel antiplatelet agent for secondary prevention in patients with a history of atherosclerotic disease: design and rationale for the thrombin-receptor antagonist in secondary prevention of atherothrombotic ischemic events (TRA 2°P)-TIMI 50 trial. *Am Heart J*. 2009;158:335–341.e3.